Surface Mounted Molecular Dipolar Rotors and Rotor Arrays

NSF Functional Nanostructures Grant 9871917

Principal Investigators:
Josef Michl, Department of Chemistry and Biochemistry, Univ. of Colorado
John Price, Department of Physics, Univ. of Colorado
Mark Ratner, Department of Chemistry, Northwestern Univ.

Collaborators:
Laura Clarke (CU Physics), Gregg Kottas (CU Chemistry), Tom Magnera (CU Chemistry)

Rotor Synthesis and Surface Mounting

Considerable effort has gone into the synthesis of rotors and their mounting on surfaces. In addition to the commercially available analogs of rotors **1** - **4** lacking the triple bond [such as $ClCH_2$-$Si(OEt)_3$], and the easily synthesized molecule **2**, all of which have small dipole moments but a small footprint, permitting high surface densities, we have worked on structures of the types **5** - **8**, with much higher dipoles. The free acetylene of **5** has been synthesized in five steps from veratrole, but the direct addition of the triethoxysilyl group needed for surface binding (to quartz) is difficult (deprotonation proceeds well but silane reagents seem to trigger phthalocyanine formation). Currently, we are synthesizing compounds **6** and **7** in a way that avoids this problem.

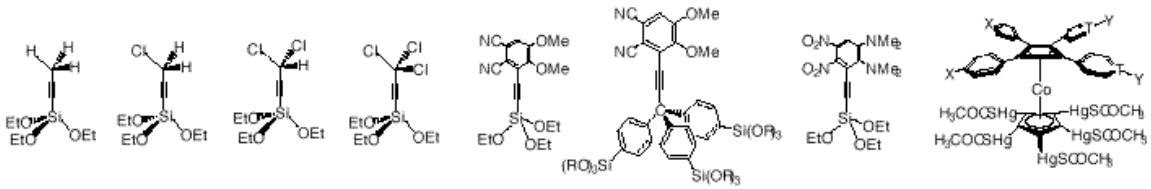

1 **2** **3** **4** **5** **6** **7** **8**

The syntheses of three rotors of type **8** have also progressed well: (1) X = NO_2, Y = NMe_2, T = C; (2) X = SO_3^-, Y = NMe_3^+, T = C; and (3) X = CH_3, Y = O, T = N. The tetraphenylcyclobutadienecobalt(I)cyclopentadienyl cores are synthesized by reaction of the appropriate diaryl acetylenes with cyclopentadienylcobalt(I)dicarbonyl in 20 - 70% yields and further derivatized as needed. Electrophilic introduction of five RHg moieties on the cyclopentadiene (Cp) ring is achieved with mercury(II)trifluoroacetate and has been accomplished directly with rotor **8**,3. Rotor **8**,1 favors substitution on the activated phenyl ring and rotor **8**,2 is not yet available easily enough to attempt this substitution. Currently, we are attempting to deactivate the anilino ring on **8**,1 to discourage substitution on the phenyl ring and working out conditions for sulfonating rotor **8,**2 from the precursor bromophenyl compound. For **8,**3 to bind to the quartz surface, alkoxysilane groups must be appended to the Cp ring. This is achieved by reacting the mercury groups with an appropriate thiol which is connected to the siloxy functionality by a hydrocarbon chain. In this way, 3-mercaptopropyltriethoxysilane was added to **8**,3-$(HgOCOCF_3)_5$ giving **8**,3-$[HgSCH_2CH_2CH_2Si(OEt)_3]_5$.

The deposition of rotors onto surfaces has been examined with the readily accessible analog of rotor **2**, diluted with **1**, both without the triple bond. The material is deposited as a vapor at 10^{-6} torr in a vacuum chamber containing quartz with lithographically patterned electrodes, bare quartz and bare silicon. The latter substrate is used to determine layer thickness by single-wavelength ellipsometry and the composition of the deposited monolayer by Auger spectroscopy.

Dielectric Relaxation Measurements on Rotor Arrays

The goal of these measurements was to study the low frequency dynamics of both interacting and non-interacting rotor arrays. For non-interacting (low density) arrays, we wished to measure the equilibrium polarization and the relaxation time. The equilibrium polarization depends on the product of the rotor density and the dipole moment per rotor, while the relaxation time depends on the barrier height for rotation and the attempt frequency. The arrays we have studied so far are disordered. At high densities (where interactions are important) we expect to see the effects of glassy behavior in both the equilibrium polarization and the relaxation response.

Measurement Technique

For electronic measurements rotor molecules analogous to **2** (without the triple bond) were incorporated into a planar capacitor with gold interdigital electrodes, patterned on a quartz glass substrate using optical lithography. The gap between the electrodes is 10 μm wide and total capacitance is about 1.2 pF. The molecular rotors are deposited from a vapor onto the glass in the spaces between the gold electrodes.

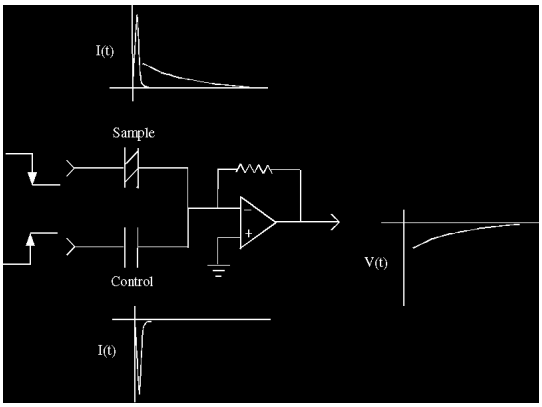

Fig. 1 Schematic diagram of the dielectric relaxation measurement apparatus.

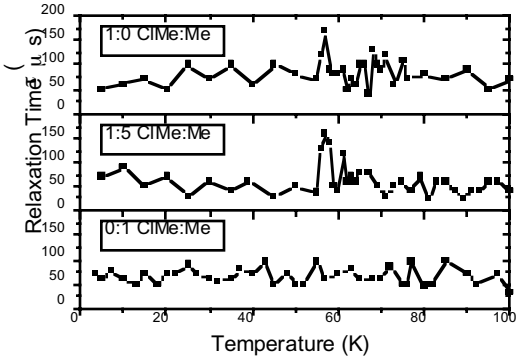

Fig 2. The polarization relaxation rate for rotors of type **2** (no triple bond). The control sample of rotors of type **1** (no triple bond) shows no peak near 60 K.

A schematic of our measurement apparatus is shown in Figure 1. We apply a 15 V potential difference across the sample capacitor for a period long enough to establish equilibrium, and then change the sign of the potential in less than 1 μs. The resulting current through the sample capacitor is shown in the upper graph. There is a prompt response due to dielectric relaxation of the substrate and then a much slower relaxation as the rotors reorient. The prompt

signal is nulled at the amplifier input by combining it with a similar response from a control capacitor. Many time-domain sweeps are averaged on a digital oscilloscope to reduce the electronic noise. Our resolution at present is about 1 fC for the total integrated charge flowing out of the sample capacitor after the voltage step is removed. The resolution is highest for relaxation times in the 50–300 μs range. The sample is located on the cold stage of a single-shot ^{3}He evaporation cryostat and its temperature can be controlled from 400 K to 0.3 K. The rotors analogous to **2** that we have studied so far are frozen out below about 30 K, but in the future we will study rotors with smaller barriers, such as **2** itself, down to lower temperatures.

For a non-interacting rotor array the integrated charge is given by

$$Q = Nd\mu L(E/2kT)$$

where N is the number of squares in the interdigital electrodes, d is the rotor area density, μ is the bare rotor dipole moment, and L is the interdigital electrode gap. The effect of thermal fluctuations is to reduce the charge by the Curie factor $E/2kT$, relative to the value for perfectly oriented rotors.

Results

In Figure 2 we show results for the relaxation times for three samples, one with a $5 \cdot 10^{18}$ m^{-2} coverage of rotors analogous to **2** (no triple bond), one with a coverage of $1 \cdot 10^{18}$ m^{-2} (obtained by dilution with non-polar methyl rotors and analogous to **1**) and a control sample with only the latter rotors. The data we display were obtained by fitting the time domain decay to two exponentials. The time constant of the slower decay is plotted. At most temperatures this is due to the background relaxation of about 50 μs, but over a narrow temperature range near 60 K the two samples with polar rotors show a much slower decay.

This narrow relaxation peak is what should be expected for non-interacting rotors with a large barrier height for rotation. The rotation is thermally activated and the relaxation rate varies rapidly with temperature, so there is a very narrow temperature range where the relaxation can be seen. If it is too fast it is lost in the electronic and background responses, and if it is too slow we do not have sufficient signal-to-noise ratio to see it. The central temperature and width of the peak correspond to an Arrhenius law with a barrier height of 1200 K and an attempt frequency of 10^{13} s^{-1}, which agrees nicely with expectations for these molecules based on a Hartree-Fock calculation on a simple model structure. The observed integrated current (proportional to equilibrium polarization) for the dilute (1:5) sample is one-third of the value expected from the rotor density, suggesting that either not all the rotors are active or our coverage estimates are in error. The observed equilibrium polarization for the full coverage sample is about 15 times smaller than expected for non-interacting rotors at that coverage. However, in this case the density is high enough that interactions are certainly important, and it may be that a large fraction of the rotors are frozen by rotor-rotor interactions. One might have expected that the full coverage sample would show slower relaxation or a broad range of decay times, but this is not observed. It may be that the observed signal reflects an inhomogeneous coverage, and comes mainly from regions of low density.

In the immediate future we hope to gain a better understanding of the density dependence of the signal for these rotors by (i) a better characterization of coverage using Auger spectroscopy (ii) improved signal-to-noise ratios from samples with larger capacitance.

Rotor Simulation - Individual Rotors

A previously NSF funded departmental computer facility, a newly adapted previously written program for the computation of classical molecular dynamics using Newton's and Coulomb's laws, and the UFF force field taken from the literature, were used to simulate the response of the rotor **9** with a large dipole moment (μ = 42 debye) and moment of inertia (1.5_10^4 uÅ^2, where u is the atomic mass unit), mounted in vacuum on a sizeable segment of a square grid polymer, to a rotating electric field. The time steps used for integration were 2.1 fs. A total of 171 dynamics runs at electric fields ranging from 100 to 7000 kV/cm in strength and from 3 to 200 GHz in frequency lasted over 100 ns. The starting temperature was 150 K, such that kT was barely above the calculated rotational barrier of ~0.3 kcal/mol, and it changed very little during a run. To evaluate the performance of the rotor, seven quantities were monitored continuously during each run, such as the rotor angular momentum and the accumulated angular lag a of the rotor behind the field (a is normalized in a way that makes a = 0 correspond to no field turns skipped, or perfect response, and a = 1 to all field turns skipped, or no response). In the absence of a driving field, the rotation of the rotor decayed in time approximately exponentially, with a relaxation time of ~80 ps.

We found that for fields that are sufficiently strong and frequencies that are sufficiently low, the rotor acts like a synchronous motor and turns with the field. At each frequency, a minimum "break-off" strength of the electric field is required (E_{bo}), below which the rotor fails to rotate at all (a = 1). Taking the value $a = 1/e$ as the maximum permissible if a rotation is to be considered perfect, we defined the critical field strength E_c to be the weakest field required to assure this condition. Classical friction and random thermal motion were identified as the two factors that oppose smooth rotation of the molecular motor. In order to provide a phenomenological characterization of the rotor in terms useful for statistical treatments of large rotor arrays, a simple model was used, based on the Arrhenius equation and containing only one adjustable parameter, namely a friction constant, allowed to be a function of frequency. This permitted an excellent fit of all the a values obtained in the simulations (within their statistical uncertainties due to limited run lengths), and produced the predictions for E_{bo} and E_c. The results have been submitted for publication (Vacek, J.; Michl, J., submitted for review in *Proc. Natl. Acad. Sci. USA*).

Rotor Simulation - Rotor Arrays

The effective transport of energy and signals in adlayer assemblies constitutes the functional heart of an entirely new approach to molecular signaling and response. After an initial study of simple longitudinal dipole chains, work on ordering, excitations and signal transport in transverse molecular dipole chains has now been completed and published (Sim, E., Ratner, M.A. and deLeeuw, S.W. *J. Phys. Chem. B*, **103**, 8663-8670). The dispersion relation for these transverse dipoles is far more similar to that for phonons than was the case in our earlier work on longitudinal dipole chains. These also support soliton-like excitations down the chain, excitations that can result in signal transport, signal processing, and addressability of remote sites at intersecting lines.